

## DESIGN OF CONTROLLED PIEZOELECTRIC ACTUATORS BY USING TOPOLOGY OPTIMIZATION

Mariana Moretti\*, Emílio C. N. Silva†

\*†School of Engineering, University of São Paulo. Av. Prof. Mello Moraes, 2231 - São Paulo, SP - Brazil, 05508-030.

\*e-mail: mamoretti@usp.br, †e-mail: ecnsilva@usp.br

**Key words:** Topology Optimization Method, Piezoactuator, Active Control Law, Time-Domain Transient Analysis.

**Abstract.** Controlled flextensional actuators essentially involve a compliant mechanism assembled in association with piezoceramics featuring sensing and actuation of the structure by the ceramics energy conversion property. For applications that require vibration response attenuation, these devices account with an active feedback control to regulate disturbances that might be introduced to the system. In the field of intelligent structures, the self-monitoring and control assemblage can be largely used in systems such as micro-grippers for sample handling, hard disk reading [1] and atomic force microscopy. One distinct advantage of this kind of structure is their higher accuracy when compared to conventional actively controlled structures because their sensing is distributed instead of being discrete about the response measurement phenomenon. The control law effectiveness in such a controlled system can be enhanced by designing their elastic structure by means of the Topology Optimization Method (TOM), since an optimized material distribution within a fixed domain affects the structure stiffness, vibration modes and response characteristics. Previous works that apply the TOM in controlled piezo-actuators aiming vibration suppression focus on the distribution of piezoceramic material over a host structure either in frequency domain or in time domain [2]. However, the low coupling constants of piezoelectric ceramics may reduce the capability of energy conversion for input displacements or for input voltages in actuating systems. Therefore, in order to avoid an unfeasible or less effective active control targeting vibration suppression, this work focuses on the distribution of the host structure and eliminates the dependence on the magnitude of electro-elastic coupling constants for a satisfactory energy conversion. As stated, the optimized smart devices proposed in this work involve a host structure material distribution which is sensed and actuated by two predefined piezoceramic locations connected through a feedback architecture, while the system is subjected to a transient input load. Approximations to the damping matrix coefficients are considered for both the metallic material and the piezoelectric material, even though the ceramic layers are significantly thinner than the middle layer. The objective function chosen minimizes the

vibration energy of the system subjected to a volume constraint. The dynamic equilibrium equation accounts with an extra damping matrix derived from the current amplification chosen as the feedback control law, or for short, the Active Velocity Feedback (AVF). The material model implemented is the Solid Isotropic Material with Penalization (SIMP) for the 4-node solid finite element with two mechanical degrees-of-freedom (DOFs) per node, and one electrical DOF per node. A density-based filter eliminates the checkerboard pattern, the sensitivity analysis is calculated by the adjoint method, and the Sequential Linear Programming (SLP) algorithm is employed as the optimization procedure. Two-Dimensions (2D) results are presented and the influence of the gain velocity value over the final layouts is analyzed.

## 1 INTRODUCTION

Refinement on motion precision of actuating systems envision applications in most of the modern electronic devices, which require lighter, less stiff and more vulnerable to transient external loads components [3]. The optical pickup system on hard drive reading, the hard drive base itself and the servovalves in hydraulic control systems are examples of devices that have their work operation based on fast response and vibration suppression actuation. Intelligent structures provide those characteristics given that their self-monitoring feature based on sensors, actuators and an active control law, interfere to the systems dynamics. Among the smart materials employed with sensing and actuation properties to regulate vibrations to the referred systems, the piezoelectric ceramic is the most commonly used of them.

Time-domain formulation for piezoelectric transducers has been studied by Wang (2001) [4], who applied the velocity feedback control and evaluated the system stability according to its piezoceramics placement, by Zhang (2015) [5], who applied LQR and PID control schemes for free vibration and step, harmonic and random excitations to study their influence on the response of flexible structures. For the previously mentioned works, the predefined placement of sensors and actuators associated with an active controller resulted in vibration attenuations of the system. An active vibration control scheme is defined by the extra voltage or electric charge that is supplied to the piezoceramic material [6]. Further improvement to these systems response might require an optimized sensor, actuator and base materials distribution, a structure design conveyed by the Topology Optimization Method (TOM).

With the advancements in processing capability of computers, the TOM have been made possible for the design of systems under dynamical analysis. Jang (2012) [7] showed that, under multiple dynamic loads, the dynamic response topology optimization substantially reduces the strain energy when compared to the static topology optimization. Deng (2014) [8] combined TOM and optimal control method to obtain the optimal match between the material distribution and the control effect applied to heat transfer, steady

flow and structure compliance problems.

Focusing on the dynamic load case scenario and on the TOM for the design of controlled piezoelectric actuators, recent works have optimized the distribution of piezoelectric patches within the structures to enhance the control effects towards a specific operation mode. Wang (2006) [9] applied a genetic algorithm-based topology optimization to the design of sensors and actuators for torsional vibration control of laminated composite plate. In the work of Zhang et al. (2014a) [10], the authors work with an optimized electrode distribution over piezoelectric sensors and actuators attached to a thin-walled shell structure for reducing sound radiation. Yet, in their most recent work, Zhang et al. (2014b) [2] used the same optimized electrode distribution applied to the vibration suppression in time-domain, assuming thin layers of piezoelectric material and therefore rejecting their damping effects.

Besides being more versatile to distribute the piezoceramic material, their low coupling constants may reduce the capability of energy conversion for input voltages in actuating systems, what results in an unfeasible problem when applied to certain active control that depends on the magnitude of electro-elastic coupling constants. In that case, for the active control to be efficient, a large control gain would be needed [11]. Therefore, this work proposes to apply the TOM to the host layer of the structure, given the locations for the sensor and actuator layers, in order to achieve better control performance with lower control gain.

Unlike most part of previous study on topology optimization, this work focuses on a time-domain transient analysis to achieve the goal of vibration suppression on piezoelectric structures. TOM is used to optimize the compliant structure for reduced vibration given two predefined locations for the ceramic layers. The TOM implementation is based on a density material model, the Solid Isotropic Material with Penalization (SIMP) and the velocity feedback control technique is chosen for the regulation. To illustrate the method, bidimensional optimized topologies of flextensional actuators are obtained considering different active control gains. The efficiency of these devices is evaluated for each of the control gains implemented.

## 2 FEM FOR A TRANSDUCER UNDER AVF CONTROL

In order to develop the closed loop equations of motion for the active controlled piezoelectric transducer, the boundary conditions of the prospective system are presented in figure 1. The solid system  $\Omega = \Omega_1 \cup \Omega_2$  is formed by the piezoelectric domain  $\Omega_1$  and the elastic domain  $\Omega_2$  inside a fixed domain  $\bar{\Omega}$  ( $\Omega \subseteq \bar{\Omega}$ ) to which constraints and loads are defined. The boundary surface of  $\bar{\Omega}$ -system, denoted by  $\Gamma$ , is partitioned into prescribed mechanical displacements  $\Gamma_u$ , prescribed traction vector  $\Gamma_T$ , an equipotential electroded region  $\Gamma_\phi$  and an unelectroded region  $\Gamma_D$ , where it concentrates the free charge density per unit surface area.

The dynamics of deformation here is approximated by a 2D-solid bilinear finite element and the displacement field  $\mathbf{U} = [\mathbf{u} \ \Phi]^\top$  is given by two mechanical components

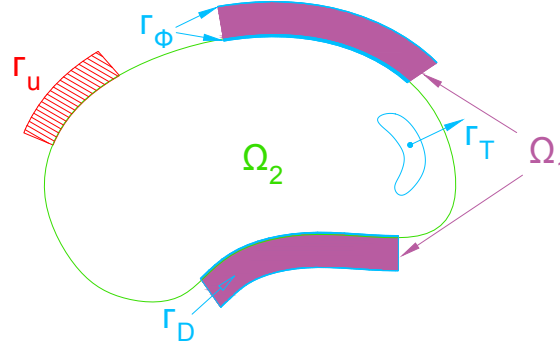


**Figure 1:** Design domain

$\mathbf{u} = [u_x \ u_y]^\top$  for deformations in directions  $x$  and  $y$ , respectively. The electric vector component  $\Phi = [\Phi_f \ \Phi_p]$  is subdivided into free voltages,  $\Phi_f$ , for intermediate nodes in ceramic layers, and prescribed voltages,  $\Phi_p$ , for electrode nodes. The grounded electrodes are not represented in the equations.

The strain-displacement field is defined by the normal strains  $S_x$  and  $S_y$  in  $x$  and  $y$  directions, respectively, and by the in-plane shear strain  $S_{xy}$ :

$$\mathbf{S} = [S_x \ S_y \ S_{xy}]^\top. \quad (1)$$

Likewise, the stress components are given by the stress vector

$$\mathbf{T} = [T_x \ T_y \ T_{xy}]^\top, \quad (2)$$

and along with the electric displacement vector  $\mathbf{D}$  and the coupling piezoelectric tensor  $\mathbf{e}$ , the piezoelectric constitutive equations are written:

$$\begin{aligned} \mathbf{T} &= \mathbf{c}^E \mathbf{S} - \mathbf{e} \mathbf{E}, \\ \mathbf{D} &= \mathbf{e} \mathbf{S} + \boldsymbol{\epsilon}^S \mathbf{E}. \end{aligned} \quad (3)$$

In the piezoelectric constitutive equations,  $\mathbf{c}^E$  is an elastic matrix evaluated under a constant electric field  $\mathbf{E}$ , and  $\boldsymbol{\epsilon}^S$  is a dielectric tensor evaluated under constant strain  $\mathbf{S}$ .

Considering infinitesimal deformation, the linear behaviour of piezoelectric materials and the linear electric and structural fields in plane stress condition result in the material

matrices given by

$$\mathbf{c}^E = \begin{bmatrix} c_{11} - \frac{c_{12}^2}{c_{11}} & c_{13} - \frac{c_{12}c_{13}}{c_{11}} & 0 \\ c_{13} - \frac{c_{12}c_{13}}{c_{11}} & c_{33} - \frac{c_{13}^2}{c_{11}} & 0 \\ 0 & 0 & c_{66} \end{bmatrix}, \quad (4)$$

$$\mathbf{e} = \begin{bmatrix} 0 & e_{31} - \frac{e_{31}c_{12}}{c_{11}} \\ 0 & e_{33} - \frac{e_{31}c_{13}}{c_{11}} \\ e_{15} & 0 \end{bmatrix}, \quad (5)$$

$$\boldsymbol{\varepsilon}^S = \begin{bmatrix} -\varepsilon_{11} & 0 \\ 0 & -\varepsilon_{33} - \frac{e_{31}^2}{c_{11}} \end{bmatrix}, \quad (6)$$

where  $c_{66} = \frac{c_{11} - c_{12}}{2}$ , [12].

The dynamic equations of motion in matrix form for a bounded piezoelectric body are derived from the Hamilton's principle for a time interval from  $t_1$  to  $t_2$ . The interpolation of the displacement field  $\{\mathbf{u}\}$  and the electric potential  $\{\Phi\}$  are done by means of the shape functions  $[\mathcal{N}_u]$  and  $[\mathcal{N}_\phi]$  for the Q4-bilinear finite element. The convenience of applying this technique to solve the piezoelectric equations for the design of optimized transducers, relies on the fact that Topology Optimization procedure is based on systematic analysis of the physical behaviour of the system. Therefore, the FEM is ideal for a design based on computational iterations so the variational formulations of mathematical models can be solved. Combining the equilibrium equations established for all elements, the system of equations in matrix form needs to be solved:

$$\begin{bmatrix} \mathbf{M}_{uu} & \mathbf{0} & \mathbf{0} \\ \mathbf{0} & \mathbf{0} & \mathbf{0} \\ \mathbf{0} & \mathbf{0} & \mathbf{0} \end{bmatrix} \begin{Bmatrix} \ddot{\mathbf{U}} \\ \ddot{\Phi}_f \\ \ddot{\Phi}_p \end{Bmatrix} + \begin{bmatrix} \mathbf{C}_{uu} & \mathbf{0} & \mathbf{0} \\ \mathbf{0} & \mathbf{0} & \mathbf{0} \\ \mathbf{0} & \mathbf{0} & \mathbf{0} \end{bmatrix} \begin{Bmatrix} \dot{\mathbf{U}} \\ \dot{\Phi}_f \\ \dot{\Phi}_p \end{Bmatrix} + \begin{bmatrix} \mathbf{K}_{uu} & \mathbf{K}_{u\phi_f} & \mathbf{K}_{u\phi_p} \\ \mathbf{K}_{u\phi_f}^\top & -\mathbf{K}_{\phi_f\phi_f} & -\mathbf{K}_{\phi_f\phi_p} \\ \mathbf{K}_{u\phi_p}^\top & -\mathbf{K}_{\phi_f\phi_p}^\top & -\mathbf{K}_{\phi_p\phi_p} \end{bmatrix} \begin{Bmatrix} \mathbf{U} \\ \Phi_f \\ \Phi_p \end{Bmatrix} = \begin{Bmatrix} \mathbf{F} \\ \mathbf{Q}_f \\ \mathbf{Q}_p \end{Bmatrix}, \quad (7)$$

knowing that the global matrices  $\mathbf{M}$ ,  $\mathbf{C}$  and  $\mathbf{K}$  are defined as below:

$$[\mathcal{M}]_e = \int_{\Omega_e} \rho_e [\mathcal{N}_u]_e^\top [\mathcal{N}_u]_e \, d\Omega_e \quad \mathbf{M}_{uu} = \sum_e [\mathcal{M}]_e \quad (8)$$

$$[\mathcal{K}_{uu}]_e = \int_{\Omega_e} [\mathcal{B}_u]_e^\top [\mathbf{c}^E]_e [\mathcal{B}_u]_e \, d\Omega_e \quad \mathbf{K}_{uu} = \sum_e [\mathcal{K}_{uu}]_e \quad (9)$$

$$[\mathcal{K}_{u\phi}]_e = \int_{\Omega_e} [\mathcal{B}_u]_e^\top [\mathbf{e}]_e^\top [\mathcal{B}_\phi]_e \, d\Omega_e \quad \mathbf{K}_{u\phi} = \sum_e [\mathcal{K}_{u\phi}]_e \quad (10)$$

$$[\mathcal{K}_{\phi\phi}]_e = \int_{\Omega_e} [\mathcal{B}_\phi]_e^\top [\boldsymbol{\varepsilon}]_e [\mathcal{B}_\phi]_e \, d\Omega_e \quad \mathbf{K}_{\phi\phi} = \sum_e [\mathcal{K}_{\phi\phi}]_e \quad (11)$$

$$[\mathcal{C}]_e = \alpha [\mathcal{M}]_e + \beta [\mathcal{K}_{uu}]_e \quad \mathbf{C}_{uu} = \sum_e [\mathcal{C}]_e \quad (12)$$

where the subscript  $e$  stands for a finite element,  $[\mathcal{B}_u]$  and  $[\mathcal{B}_\phi]$  defines the derivatives of shape functions and  $\alpha$  and  $\beta$  are Rayleigh's coefficients for proportional damping. The damping matrix  $\mathbf{C}_{uu}$  involves the damping effect of the metallic layer and the piezoelectric layers.

For the control problem formulation to be stated, the boundary condition for the electrode on the sensor layer, top ceramic layer identified by  $s$ , is that its electrical voltage is null,  $\Phi_p^s = 0$ , so we can measure its nodal electrical charge  $\mathbf{Q}_p^s$ . Meanwhile, the boundary condition for the actuator layer, bottom ceramic layer identified by  $a$ , is that its input voltage is prescribed and identified by  $\Phi_p^a$ . Additionally, the electric charges at the piezoelectric internal nodes  $\mathbf{Q}_f$  are null, and the controlled transducer problem to be designed is illustrated in Figure 2

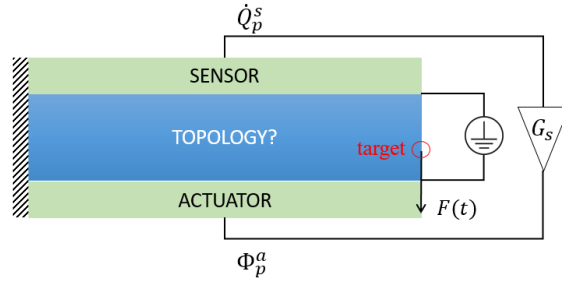


**Figure 2:** Controlled transducer with metallic layer to be designed by TOM.

Therefore, the system of equations (7) is rewritten so the electrical charges  $\mathbf{Q}_p^s$  is given as a function of the vector  $\mathbf{U}$ . Given the aforementioned boundary conditions, the electric potential vector on the ceramic internal nodes is defined by

$$\Phi_f = \mathbf{K}_{\phi_f \phi_f}^{-1} \mathbf{K}_{u \phi_f}^\top \mathbf{U}. \quad (13)$$

By substituting  $\Phi_f$ , equation (13), into the two other equations of the system (7), the output forces  $\mathbf{F}$  and the measured charges  $\mathbf{Q}_p^s$  at the sensor layer are given by the expressions:

$$\mathbf{F} = \mathbf{M}\ddot{\mathbf{U}} + \mathbf{C}\dot{\mathbf{U}} + \underbrace{\left( \mathbf{K}_{uu} + \mathbf{K}_{u \phi_f} \mathbf{K}_{\phi_f \phi_f}^{-1} \mathbf{K}_{u \phi_f}^\top \right)}_{\mathbf{H}_{uu}} \mathbf{U}, \quad (14)$$

$$\mathbf{Q}_p^s = \underbrace{\left( \mathbf{K}_{u \phi_p^s}^\top - \mathbf{K}_{\phi_f \phi_p^s}^\top \mathbf{K}_{\phi_f \phi_f}^{-1} \mathbf{K}_{u \phi_f}^\top \right)}_{\mathbf{H}_{u \phi_p^s}^\top} \mathbf{U}. \quad (15)$$

Based on the voltage definition for a current amplifier, the sensor output charges  $\mathbf{Q}_p^s$  are differentiate in time and multiplied by a constant gain  $G_s$  to obtain the sensor voltage output

$$\Phi_p^s = G_s \mathbf{H}_{u \phi_p^s}^\top \dot{\mathbf{U}}. \quad (16)$$

Premultiplying equation (16) by a unit vector  $\mathbf{I} = \{1 \dots 1\}$ , of the electrode sensor layer nodal size  $\phi_p^s$ , a scalar output voltage  $\varphi$  is obtained. In order to have an equipotential input voltage to the actuator electrode,  $\varphi$  must multiply a unit vector  $\mathbf{I}^\top$  on the actuator electrode nodal size  $\phi_p^a$ . Therefore,

$$\Phi_p^a = G_s \mathbf{I}_{\phi_p^a} \mathbf{I}_{\phi_p^s} \mathbf{H}_{\phi_p^s u} \dot{\mathbf{U}}. \quad (17)$$

Rewriting the dynamical system (7) in  $H$ -matrix form with equation (17) based on previous developments, the equation to be solved by a time integration method is stated:

$$\begin{bmatrix} \mathbf{M}_{uu} & \mathbf{0} \\ \mathbf{0} & \mathbf{0} \end{bmatrix} \begin{Bmatrix} \ddot{\mathbf{U}} \\ \ddot{\Phi}_f \end{Bmatrix} + \begin{bmatrix} \mathbf{C}_{uu} - G_s \mathbf{K}_{u\phi_p^a} \mathbf{I}_{\phi_p^a} \mathbf{I}_{\phi_p^s} \mathbf{H}_{\phi_p^s u} & \mathbf{0} \\ G_s \mathbf{K}_{\phi_f \phi_p^a} \mathbf{I}_{\phi_p^a} \mathbf{I}_{\phi_p^s} \mathbf{H}_{\phi_p^s u} & \mathbf{0} \end{bmatrix} \begin{Bmatrix} \dot{\mathbf{U}} \\ \dot{\Phi}_f \end{Bmatrix} + \begin{bmatrix} \mathbf{K}_{uu} & \mathbf{K}_{u\phi_f} \\ \mathbf{K}_{u\phi_f}^\top & -\mathbf{K}_{\phi_f \phi_f} \end{bmatrix} \begin{Bmatrix} \mathbf{U} \\ \Phi_f \end{Bmatrix} = \begin{Bmatrix} \mathbf{F} \\ \mathbf{0} \end{Bmatrix}. \quad (18)$$

Therefore, equation (18) is the FE system for the transient velocity feedback analysis.

### 3 THE TOM FOR AN AVF CONTROL LAW

The TOM has been employed to design smart structures based on piezoelectric material such as actuators [13] and transducers [14] for a static or quasi-static analysis. In the field of intelligent structures, the topology optimization has been first applied in combination with a velocity feedback control by Zhang [2] and [5], who implemented an objective function based on the measurements of the displacement on a target degree of freedom.

In this work, TOM aims to extremize an objective function for a structure under a transient load and a velocity feedback control. It employs a material model concept [15] to distribute void and solid within a design domain aiming to extremise a cost function, and uses the FEM for systematic structure analysis. The SIMP is the material model employed in this work.

For the vibration suppression purpose, the objective function defined in this work considers the minimization of a energy function involving the velocity of a target point,  $\dot{u}_{\text{dof}}$ . The design variables vector is the pseudodensity  $\rho$  of the host layer at each finite element, while a volume constraint  $V_{\text{max}}$  limits the material distribution for the design of a lightweight flexible structure with joints optimally located as to condense the ceramics displacements.

Therefore, the objective function defined monitors the vibration response over a given time interval  $[0, t_f]$  as follows:

$$f = \int_0^{t_f} g(\dot{\mathbf{U}}(t, \boldsymbol{\rho})) dt. \quad (19)$$

The function  $g(\dot{\mathbf{U}}(t, \boldsymbol{\rho}))$  may be defined to monitor several types of structural behaviour, but here the objective function is to reduce the structure vibration by spanning in time the velocity  $\dot{u}_{\text{dof}}$  of a target degree of freedom:

$$g(\dot{\mathbf{U}}(t, \boldsymbol{\rho})) = \dot{\mathbf{U}}^\top \mathbf{B} \dot{\mathbf{U}}, \quad (20)$$

where  $\mathbf{B} = \mathbf{B}^\top$  is used to specify the target degree of freedom. It is a null matrix where its diagonal equals 1 only at the target dof.

The optimization problem is stated bellow for the modified damping matrix of the system (18) represented by  $\mathbf{C}_{tm}$ :

$$\begin{aligned} \min_{\boldsymbol{\rho}} f(\boldsymbol{\rho}) &= \int_0^{t_f} \dot{\mathbf{U}}^\top \mathbf{B} \dot{\mathbf{U}} dt \\ \text{s.t.} \quad &\begin{cases} \mathbf{M}(\boldsymbol{\rho})\ddot{\mathbf{U}} + \mathbf{C}_{tm}(\boldsymbol{\rho})\dot{\mathbf{U}} + \mathbf{K}(\boldsymbol{\rho})\mathbf{U} = \mathbf{F}(t) \\ \dot{\mathbf{U}}|_{t=0} = \dot{\mathbf{U}}_0 \\ \mathbf{U}|_{t=0} = \mathbf{U}_0 \\ \sum_{e=1}^{N_e} \rho_e V_e \leq V_{\max} \\ 0 < \rho_{\min} \leq \rho_e \leq 1 \end{cases} \end{aligned} \quad (21)$$

As a solid and void profile is desired, the penalization factor  $q$  of the SIMP model accounts with smooth increments along each iteration of the TOM. Denominated the continuation approach, this procedure prevents a premature convergence to a local minima.

Therefore, the element elasticity tensor  $c_{ijkl}^n$ , for a basic isotropic metallic material  $c_{ijkl}^E$  and void-property material  $c_{ijkl}^0$ , is given by

$$\mathbf{c}(\rho_n) = \rho_n^q(x_c, y_c) \mathbf{c}^E + (1 - \rho_n^q(x_c, y_c)) \mathbf{c}^0, \quad (22)$$

where  $(x_c, y_c)$  is the finite element Cartesian centroid coordinate pair.

#### 4 NUMERICAL IMPLEMENTATION

The steps involved in the topology optimization algorithm are described in the flow chart shown in Figure 3.

The software was implemented in MATLAB with an optimization solver based in the Sequential Linear Programming (SLP), which has proved to be efficient for the kind of problem therein proposed. As a gradient-based mathematical programming algorithm, the SLP needs the sensitivity analysis of the objective function with respect to the design variables, which is calculated through the adjoint function in place of the original objective function as stated below:

$$\mathcal{L}(\dot{\mathbf{U}}, \boldsymbol{\lambda}) = \int_0^{t_f} g(\dot{\mathbf{U}}(t, \boldsymbol{\rho})) dt + \int_0^{t_f} \boldsymbol{\lambda}^\top(t) \left[ \mathbf{M}(\boldsymbol{\rho})\ddot{\mathbf{U}} + \mathbf{C}_{tm}(\boldsymbol{\rho})\dot{\mathbf{U}} + \mathbf{K}(\boldsymbol{\rho})\mathbf{U} - \mathbf{F}(t) \right] dt. \quad (23)$$

Taking the derivative of the Lagrangian (23) with respect to the design variables  $\boldsymbol{\rho}$  we

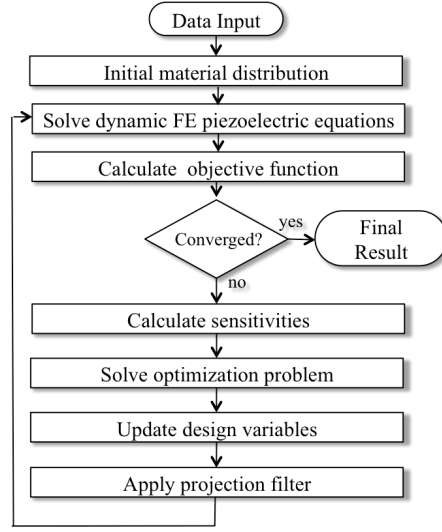


**Figure 3:** Flowchart of the implemented optimization procedure.

get the final valued adjoint problem

$$\begin{cases} M\ddot{\lambda}^\top(t) - C_{tm}\dot{\lambda}^\top(t) + K\lambda^\top(t) = \frac{d}{dt} \left( \frac{\partial g}{\partial \dot{U}} \right) \Big|_t \\ \lambda^\top(t_f) = \mathbf{0} \\ \dot{\lambda}^\top(t_f) = M^{-1} \frac{\partial g}{\partial \dot{U}} \Big|_{t_f} \end{cases}, \quad (24)$$

and to obtain the initial value primal problem, a change of variable is applied  $\tau(t) = t_f - t$ :

$$\begin{cases} M\ddot{\Lambda}^\top(\tau(t)) + C_{tm}\dot{\Lambda}^\top(\tau(t)) + K\Lambda^\top(\tau(t)) = 2B\ddot{U} \Big|_{\tau(t)} \\ \Lambda^\top(0) = \mathbf{0} \\ \dot{\Lambda}^\top(0) = -2M^{-1} B\dot{u} \Big|_{t_f} \end{cases}. \quad (25)$$

Recalling that  $\dot{\Lambda}(\tau(t)) = -\dot{\lambda}(t)$ , the sensitivity expression for the transient problem reduces to:

$$\frac{\partial \mathcal{L}(\dot{U}, \Lambda)}{\partial \rho_e} = \int_0^{t_f} \Lambda^\top(t_f - t) \left[ \frac{\partial M(\rho)}{\partial \rho_e} \ddot{U} + \frac{\partial C_{tm}(\rho)}{\partial \rho_e} \dot{U} + \frac{\partial K(\rho)}{\partial \rho_e} U - \frac{\partial F(t)}{\partial \rho_e} \right] dt. \quad (26)$$

As it is seen by equation (26), the sensitivity analysis of this transient optimization problem involves the solution of two second order linear equations, one in  $\Lambda$  and the other one in  $U$ . Their numerical solutions are obtained by the *a*-form of Newmark's numerical integration scheme [16].

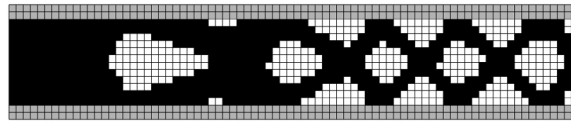


Figure 4: Optimized topology design for  $G_s = 0$

## 5 PRELIMINARY RESULTS

Given a solid initial domain of  $2\text{cm} \times 0.4\text{cm}$ , this domain is discretized by a  $80 \times 16$  finite elements with a pseudodensity vector initially set to  $\rho = 1$  at the metallic layer, restricted to  $V_{\max} = 0.7$ . The optimization problem, equation (21), was evaluated for a null feedback gain and for a feedback gain  $G_s = 10000$ .

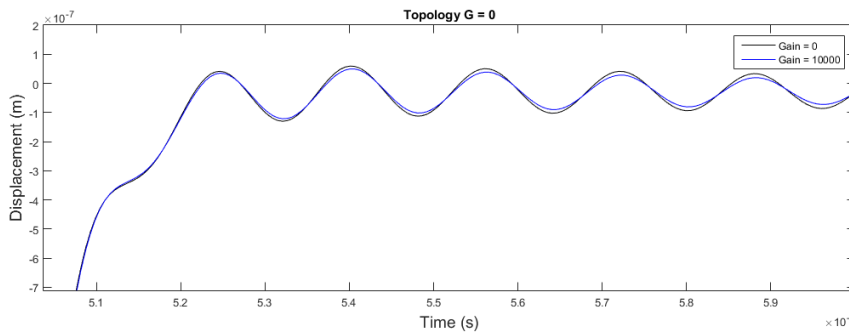


Figure 5: Target displacement for  $G_s = 0$  optimized topology

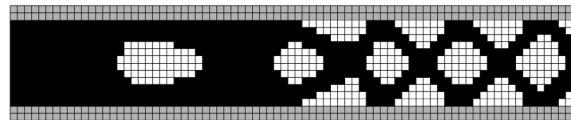
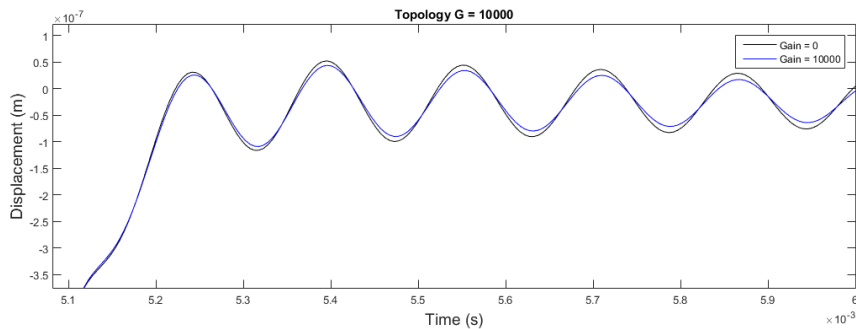


Figure 6: Optimized topology design for  $G_s = 10000$

For both simulations, the objective function converged, and from figures 5 and 7 it can be seen that the transient finite element analysis results in a lower vibration amplitude in the presence of a control gain. However, the attenuation obtained for the topology resulted from the optimization that is coupled with a control gain, Figure 6, is increased when compared with the topology resulted from the optimization with null gain, Figure 4, what in terms of objective function values represents an improvement of 1.65%.

## 6 CONCLUSIONS

The TOM was applied to the design of a vibrational structure controlled by two piezoceramic layers aiming to reduce its displacement in time. The SIMP material model was



**Figure 7:** Target displacement for  $G_s = 10000$  optimized topology

adopted and the optimization problem was solved with a Sequential Linear Programming (SLP) algorithm. The results show that to the velocity feedback gain chosen the optimization problem converges, and the final topology indicates a better improvement in response attenuation for the gain to which the structure was designed. In future work, formulation will be revised in order to obtain even greater vibration suppression in the presence of an active control feedback.

## REFERENCES

- [1] Kim, W., Song, Y. H. and Kim, J. E. *Topology optimization of actuator arms in hard disk drives for reducing bending resonance-induced off-tracks*. Structural and Multidisciplinary Optimization, Vol. 46, (2012) 6:907–912.
- [2] Zhang, X. and Kang, Z. *Dynamic topology optimization of piezoelectric structures with active control for reducing transient response*. Computer Methods in Applied Mechanics and Engineering, Vol. 281, (2014) 200-219.
- [3] Ou, J. and Kikuchi, N. *Integrated optimal structural and vibration control design*. Structural optimization, Vol. 12, (1996) 4:209–216.
- [4] Wang, S. Y., Quek, S. T. and Ang, K. K. *Vibration control of smart piezoelectric composite plates*. Smart materials and Structures, Vol. 10, (2001) 4:637–.
- [5] Zhang, S., Schmidt, R. and Qin, X. *Active vibration control of piezoelectric bonded smart structures using PID algorithm*. Chinese Journal of Aeronautics, Vol. 28, (2015) 1:305–313.
- [6] Takezawa, A., Makihara, K., Kogiso, N. and Kitamura, M. *Layout optimization methodology of piezoelectric transducers in energy-recycling semi-active vibration control systems*. Journal of Sound and Vibration, Vol. 333, (2014) 2:327–344.

- [7] Jang, H. H., Lee, H. A., Lee, J.Y. and Park, G.J. *Dynamic response topology optimization in the time domain using equivalent static loads*. AIAA journal, Vol. 50, (2012) **1**:226–234.
- [8] Deng, Y., Liu, Z., Liu, Y., and Wu, Y. *Combination of topology optimization and optimal control method*. Journal of Computational Physics, Vol. 257, (2014) -:374–399.
- [9] Wang, S. Y., Tai, K. and Quek, S. T. *Topology optimization of piezoelectric sensors/actuators for torsional vibration control of composite plates*. Smart materials and Structures, Vol. 15, (2016) **2**:253–.
- [10] Zhang, X., Kang, Z., and Li, M. *Topology optimization of electrode coverage of piezoelectric thin-walled structures with CGVF control for minimizing sound radiation*. Structural and Multidisciplinary Optimization, Vol. 50, (2014) **5**:799–814.
- [11] Ray, M. C., and Reddy, J. N. *Optimal control of thin circular cylindrical laminated composite shells using active constrained layer damping treatment*. Smart Materials and Structures, Vol. 13, (2003) **1**:64–.
- [12] Tiersten, H.F. *On the nonlinear equations of thermo-electroelasticity*. International Journal of Engineering Science, Vol. 9, (1971) **7**:587–604.
- [13] Kögl, M., and Silva, E. C. N. *Topology optimization of smart structures: design of piezoelectric plate and shell actuators*. Smart materials and Structures, Vol. 14, (2005) **2**:387–.
- [14] Silva, E. C. N. and Kikuchi, N. *Design of piezoelectric transducers using topology optimization*. Smart Materials and Structures, Vol. 8, (1999) **3**:350–.
- [15] Rozvany, G. I. N. *Aims, scope, methods, history and unified terminology of computer-aided topology optimization in structural mechanics*. Structural and Multidisciplinary Optimization, Vol. 21, (2001) **2**:90–108.
- [16] Hilber, H. M., Hughes, T. J. R. and Taylor, R. L. *Improved numerical dissipation for time integration algorithms in structural dynamics*. Earthquake Engineering & Structural Dynamics, Vol. 5, (1977) **3**:283–292.